THE JOURNAL OF PHYSICAL CHEMISTRY C

Article

pubs.acs.org/JPCC

Fumaronitrile-Based Fluorogen: Red to Near-Infrared Fluorescence, Aggregation-Induced Emission, Solvatochromism, and Twisted Intramolecular Charge Transfer

Xiao Yuan Shen,[†] Wang Zhang Yuan,[‡] Yi Liu,[†] Qiuli Zhao,[†] Ping Lu,[§] Yuguang Ma,[§] Ian D. Williams,[‡] Anjun Qin,[†] Jing Zhi Sun,*[,†] and Ben Zhong Tang*[,†,‡]

[†]Institute of Biomedical Macromolecules, Department of Polymer Science and Engineering, MoE Key Laboratory of Macromolecule Synthesis and Functionalization, Zhejiang University, Hangzhou 310027, China

[‡]Department of Chemistry, Institute of Molecular Functional Materials, The Institute for Advanced Study (IAS), The Hong Kong University of Science & Technology, Clear Water Bay, Kowloon, Hong Kong, China

[§]State Key Lab Supramolecular Structure & Materials, Jilin University, Changchun 130012, China

Supporting Information

ABSTRACT: By integrating *N*,*N*-dimethyl (donor, D) and fumaronitrile (acceptor, A) groups with the biphenyl fluorogen, which has an aggregation-induced emission (AIE) property, we have obtained the target molecule 2-(4-bromophenyl)-3-(4′-(dimethylamino)-biphenyl-4-yl) fumaronitrile (BDABFN). BDABFN is a red-to-near-infrared-emitting fluorogen with emission peaks at 653 and 710 nm for its amorphous and crystal solids, respectively. BDABFN shows an evident aggregation-induced emission property, and the fluorescence quantum efficiency of its solid is 26.5%. Cystallographic data indicate that there is no $\pi-\pi$ stacking, and neither *J*- nor *H*-aggregates are observed between the adjacent molecules. The existence of multiple C−H···π bonds between the adjacent molecules restricts the intramolecular rotation of the D and A moieties and enables the fluorogen to emit intensely in the solid states. Meanwhile, because of strong intramolecular D−A interaction, BDABFN exhibits pronounced solvatochromism, and the fluorescence peak red-shifts from 552 nm in hexane (nonpolar and hydrophobic solvent) to 750 nm in tetrahydrofuran (polar and hydrophilic solvent. BDABFN also displays a typical twisted intramolecular charge transfer property in polar solvents because of the interaction between the *N*,*N*-dimethyl and fumaronitrile moieties.

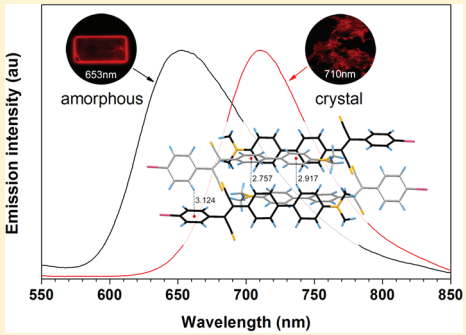

INTRODUCTION

Red-emitting materials are highly demanding in the fields of electroluminescent devices, biological imaging, and fluorescent probes.[1−7] Red fluorescence comes from fluorogens with a narrow band gap, which is achieved either by large, fused, conjugated systems or by attachment of strong electron donor (D) and acceptor (A) groups on fluorogens. Most of these molecules, however, suffer from the notorious aggregation-caused emission quenching (ACQ) effect. They emit strong fluorescence in dilute solution, but become weakly emissive in the aggregate state unless *J*-aggregates are formed.[8,9] Intermolecular $\pi-\pi$ stacking in extended π-conjugated systems and dipole−dipole interaction D−A charge transfer systems are ascribed to fluorescence quenching.[10−18] The ACQ effect heavily limits their applications in real-world situations. For example, when they are used as fluorescent probes to detect biological molecules or specific ions in buffers, the hydrophobic nature of the fluorophores makes them prone to form aggregates in aqueous media, although hydrophilic groups can be attached to the fluorophores by rational molecular design.[19] When these molecules are used as organic light-emitting diodes (OLEDs), the ACQ effect limits their roles only as dopants. Doped materials are much more difficult to control because of the low optimum doping concentration and the narrow effective doping range.[20]

An exactly opposite effect was reported by Tang and colleagues.[21] It was found that 1-methyl-1,2,3,4,5-pentaphenylsilole molecules were hardly emissive in solutions, but their aggregates or solid states were strongly luminescent. This phenomenon is termed aggregation-induced emission (AIE). Lately, AIE fluorogens have been successfully put into application in the construction of OLEDs,[22−25] bioimaging systems,[26,27] and chemical sensors.[28−34] A series of control experiments revealed that the restriction of intramolecular rotations (RIR) process is responsible for the AIE effect: the nonemission of silole in solution is attributed to the active intramolecular rotations of multiple phenyl rings on its periphery, whereas the efficient luminescence in the aggregate state is caused by the restriction of intramolecular rotations of these phenyl rings.[35] On the basis of the understanding of RIR mechanism, many different kinds of AIE molecules have been

Received: March 31, 2012
Published: April 24, 2012

synthesized,[36−39] some of which are composed of multiple aromatic peripheral rotors and classical ACQ cores, including naphthalene, anthracene, phenanthracene, pyrene, triphenylamines, and carbazole.[40−43] Particularly, tetraphenylethenoid-modified perylene bisimide and benzo-2,1,3-thiadiazole have been shown to be red-emissive.[44,45]

Cyano and *N*,*N*-dialkyl (or phenyl) moieties are commonly used as acceptor and donor to construct red-emitting fluorogens. For example, Park et al. reported strong emission from the nanoparticles of 1-cyano-trans-1,2-bis-(4′-methylbiphenyl) ethylene (CN-MBE). They attributed the observed AIE behavior to the synergetic effect of intramolecular planarization and *J*-aggregation of CN-MBE molecules in nanoparticles.[46] Tsutsui et al. reported an efficient red-electroluminescent device based on a D−A compound of 1,4-bis(1-cyano-2-(4-(N-4-methoxyphenyl-N-1,4-bis(1-cyano-2-(4-(N-4-methoxy-phenyl-N-phenylamino)phenyl)vinyl)benzene (D-CN).[47] Tao et al. reported a kind of red emitting compounds of fluorenonearylamine derivatives, which are highly fluorescent in solid-state.[48] Chen et al. reported a bright and efficient nondoped red organic light-emitting diodes employing bis(4-(N-(1-naphthyl)phenylamino)phenyl)-fumaronitrile.[49] We have recently altered green emitting silole core to efficient yellow and red emitting derivatives by linking to *N*,*N*-diphenyl and malononitrile moieties, respectively.[50,51] Herein, we report an efficient red emitter with rather simple molecular structure, in which *N*,*N*-dimethylaniline and aromatic fumaronitrile have been used as the donor and acceptor to construct the target of 2-(4-bromophenyl)-3-(4′-(dimethylamino)-biphenyl-4-yl) fumaronitrile (BDABFN), which shows strong solvatochromism, evident twisted intramolecular charge transfer (TICT) progress, and AIE activity.

RESULTS AND DISCUSSION

Fluorogen Preparation. BDABFN was synthesized in a facile synthetic route (Scheme 1). The experiment details and structure characterization data are described in the Supporting Information (SI). In brief, the target molecule was derived from the coupling of *N*,*N*-dimethyl-4-(4,4,5,5-tetramethyl-1,3,2-dioxaborolan-2-yl) aniline (**2**) and bis(4-bromophenyl)-fumaronitrile (**4**) under typical Suzuki reaction conditions. By proper control of the reactant ratio, only one of the two bromide atoms on **4** can react with **2** and gives rise to BDABFN in a good yield of 62.7%. The bromo on BDABFN can be used as an active site to couple with different conjugated moieties and to prepare different derivatives. BDABFN shows high thermal stability, with a T_d at 289 °C (SI Figure S1, the temperature at which the compound lost 5% of its weight). Solubility experiments indicate that BDABFN is highly soluble in polar and nonpolar, hydrophobic, and hydrophilic organic solvents.

Scheme 1. Synthetic Routes and Chemical Structures of BDABFN

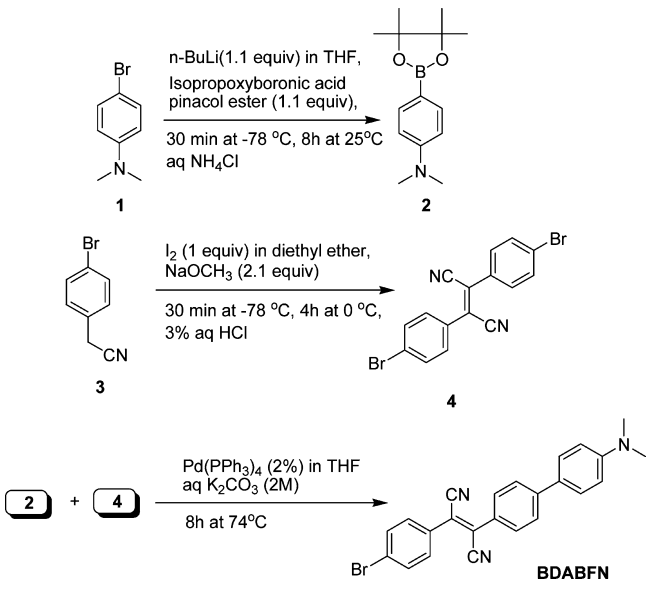

Solvatochromism. The broad-range solubility offers us a good chance to study the optical properties of BDABFN in the solvents of varying polarities. When excited by UV light, the solutions of BDABFN in nonpolar hydrophobic solvents, such as hexane and cyclohexane, emit strong yellow light, whereas the solutions emit bright red light in toluene and dark red light in 1,4-dioxane. In low-polar solvent chloroform, the emission becomes weak, and in moderate (e.g., ethyl acetate and tetrahydrofuran, or THF) and high (e.g., acetonitrile, ethanol, and methanol) polar solvents, the emission becomes nearly invisible with the naked eye (Figure 1A). The changes in the emission features of the BDABFN solutions have been quantitatively evaluated by fluorescence spectroscopy (Figure 1B). A dramatic red shift of the emission peak from 552 to 750 nm was recorded with the change in solvent polarity and hydrophobic property. In contrast, the UV−vis absorption spectra display little change with the change in solvent polarity. The absorption peaks (λ_{ab}) appear at around 437−445 nm (Figure 1C).

The effects of solvents on the emission features have been further evaluated by the relationship between the solvent polarity parameter (Δf) and the Stokes shift of the absorption and emission maxima (Lippert−Mataga equation, 1),[52,53] and the experiment data are summarized in Table 1. In hexane ($\Delta f \approx 0$), BDABFN shows a single, narrow emission peak (λ_{em}) at 552 nm, and its cyclohexane solution gives a similar emission feature with a peak at 559 nm. Although the Δf value (0.014) of toluene is only slightly higher than that of hexane, the λ_{em} is already shifted to the red spectral region (640 nm). The $\pi-\pi$ reaction between BDABFN and toluene may be a cause of this large red shift. 1,4-Dioxane, which has a Δf value (0.021) close to that of toluene, is used too. The λ_{em} is recorded at 666 nm, but the emission intensity is weaker than that in toluene, suggesting polarity may be the dominant reason for the large red shift. In chloroform, the peak is further red-shifted, and the intensity drops accordingly. When in polar solvent ethyl acetate or THF, the peak shifts to the near-infrared region (750 nm), with a dramatic decrease in the emission intensity, and in highly polar solvents acetonitrile or methanol, no emission can be recorded. These results indicate that the fluorescence behavior of BDABFN is intensely sensitive to solvent polarity, exhibiting strong solvatochromism.

$$\Delta f = f(\varepsilon) - f(n^2) \approx \frac{\varepsilon - 1}{2\varepsilon + 1} - \frac{n^2 - 1}{2n^2 + 1} \quad (1)$$

Twisted Intramolecular Charge Transfer Process. The data in Table 1 indicate the quantum yield of BDABFN in solution also shows a trend of decreasing with an increase in the solvent polarity, ranging from 0.293 in toluene to 0 in

dx.doi.org/10.1021/jp303100a | J. Phys. Chem. C 2012, 116, 10541−10547

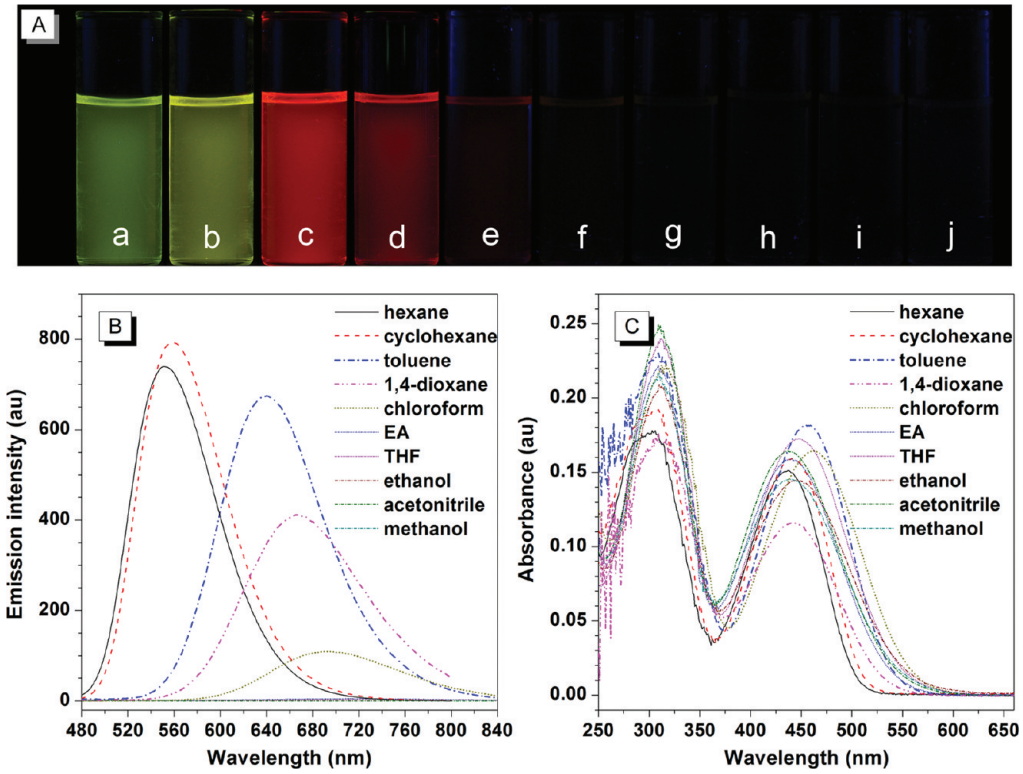

Figure 1. (A) Photographs showing the emission colors of BDABFN in different solvents (taken under UV light, from a to j are hexane, cyclohexane, toluene, 1,4-dioxane, chloroform, ethyl acetate, THF, ethanol, acetonitrile, and methanol, respectively). (B) Fluorescence spectra of BDABFN in different solvents. Solutions were excited at their absorption maxima (Table 1). (C) UV−vis spectra of BDABFN in different solvents. Concentration of BDABFN in all cases: 10 μM.

Table 1. Optical Transitions of BDABFN in Different Solvents[a]

solvent	Δf	λ_{ab} (nm)	λ_{em} (nm)	Stoke's shift (nm)	Φ_F (%)
hexane	~0	437	552	115	27.3
cyclohexane	~0	443	559	116	27.7
toluene	0.014	455	640	185	29.3
1,4-dioxane	0.021	443	666	223	12.9
chloroform	0.149	463	690	227	4.8
ethyl acetate	0.201	441	720	279	0.4
THF	0.210	445	750	305	0.4
ethanol	0.288	445	n.d.		0
acetonitrile	0.306	437	n.d.		0
methanol	0.309	441	n.d.		0

[a]Abbreviations: λ_{ab} = absorption maximum, λ_{em} = emission maximum, Φ_F = fluorescence quantum yield [estimated by using Rhodamine B as standard (Φ_F = 70% in ethanol)], and n.d. = not detectable (signal too weak to be accurately determined). Emission spectra were measured by exciting the solutions (10 μM) at their absorption maxima.

methanol. The lower quantum yield of BDABFN in higher polar media may be attributed to the formation of a TICT state that acts as a nonradiative decay.[54] Molecules with TICT properties are always characterized by large molecular dipoles and a pronounced asymmetric electron population in the frontier molecular orbitals. These characteristics are confirmed by theoretical calculation results (SI Table S1). As shown in SI Figure S2, the electron cloud in the HOMO level localizes mainly on the *N*,*N*-dimethylaniline unit, whereas that of the LUMO level locates predominantly on the fumaronitrile unit. The dipole moment is calculated to be 6.66 D. These calculation results predict the strong electron transfer in the BDABFN molecule.

To get more information about the TICT progress in a BDABFN system, we systematically changed the polarity by admixing polar THF and nonpolar hexane with different hexane fractions (f_h), then we measured the emission spectra of BDABFN in the solvent mixtures. When f_h increased from 0 to 40%, the spectra were almost flat lines parallel to the abscissa. When f_h changed from 50 to 80%, the spectra continuously blue-shifted in red region, and the emission intensity gradually increased. When f_h was above 80%, the emission color underwent further hypsochromically shift by increasing f_h, in the order of red → orange → yellow → yellow-greenish → green (Figure 2A). Simultaneously, the emission became stronger (Figures 2B and C).

AIE Behavior. In our previous work, we found a group of AIE luminogens, or BODIPY derivatives, whose emissions extend into the red light region, by taking advantage of their TICT processes.[55] For BDABFN, the unit biphenyl itself is an AIE active near-UV emitter. on the basis of the rationale of our molecular design and the experimental data demonstrated above, BDABFN is expected to be a TICT luminogen with AIE property. We examined the emission behavior of BDABFN aggregates formed in THF/water mixtures because it is soluble in all common organic solvents but insoluble in water, and BDABFN molecules must aggregate in THF/water mixtures with a high water fraction (f_w). The recorded spectra and the plot of extracted emission data are displayed in Figure 3A and B, respectively. BDABFN emits a very weak near-infrared light with a peak at 750 nm in pure THF. When water is added, the emission disappears, owing to the quick increase in the solvent

dx.doi.org/10.1021/jp303100a | J. Phys. Chem. C 2012, 116, 10541−10547

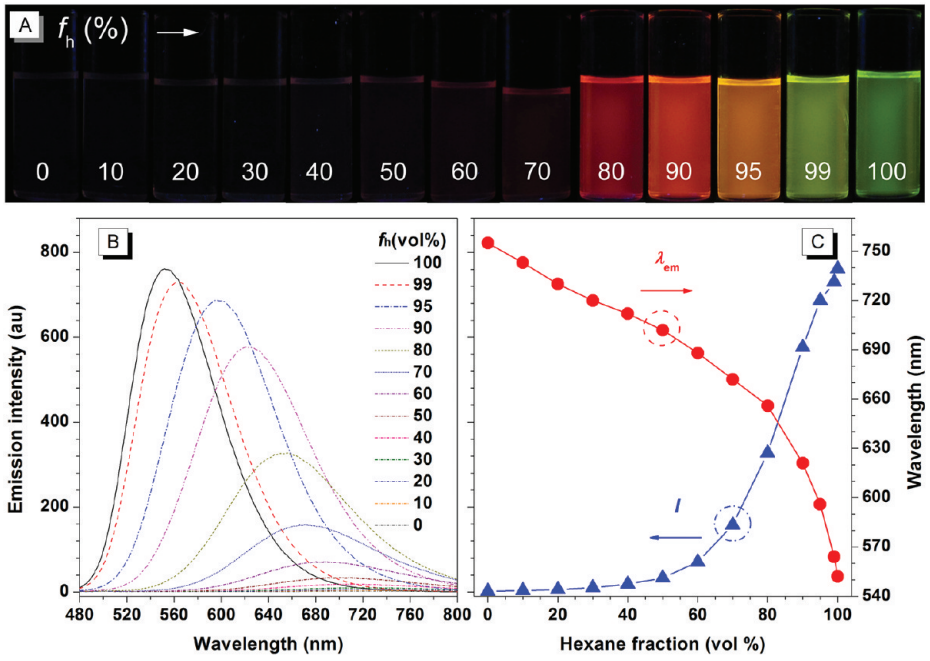

Figure 2. (A) Photographs of BDABFN in hexane/THF mixtures taken under UV illumination. (B) Fluorescence spectra of BDABFN in a hexane/THF mixture. (C) Plots of maximum emission intensity (I) and wavelength (λ_{em}) of BDABFN versus hexane fraction (f_h, vol %) in a hexane/THF mixture. Concentration of BDABFN: 10 μM. Excitation wavelength: 437 nm.

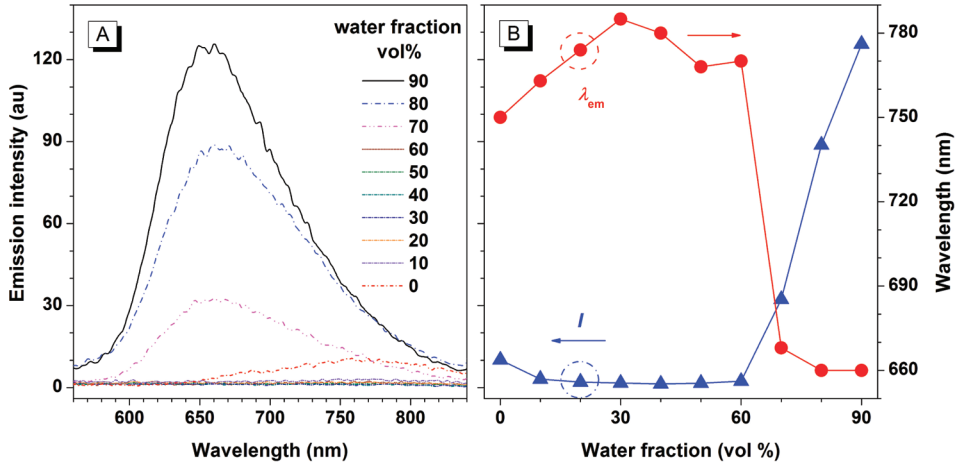

Figure 3. (A) Photoluminescence spectra of BDABFN in the water/THF mixtures. (B) Plot of maximum emission intensity (I) and wavelength (λ_{em}) of BDABFN versus water fraction. Concentration of BDABFN: 10 μM.

polarity. When f_w is above 30%, the emissions blue-shift, and theintensity is still very low. The solutions are not emissive until f_w is up to 70%. The emission is abruptly recovered at higher f_w (>70%). At the same time, the emission peak blue-shifts to 660 nm. The emission is further enhanced by further increases in f_w. At a f_w of 90%, the fluorescence intensity is 12 times greater than that in pure THF.

We also studied the emission behavior of BDABFN in the solid state. Fluorescent spectra and photographs under UV light are given in Figure 4. The emission peaks of amorphous film and single crystal samples of BDABFN are recorded at 653 and 710 nm, respectively. Intermolecular interactions may be the cause of the evident red shift of crystal emission relative to an amorphous sample. Comparing the emission behavior of solid BDABFN with its 90% THF/water mixture, the emission peaks of the BDABFN aggregates in the aqueous mixture are blue-shifted by several nanometers, and the intensity is much weaker than that of the BDABFN solid because of the solvent polarity effect in the aqueous media.[50] The fluorescence quantum yield of the BDABFN solid is 0.265, measured by using an integrating sphere. On the CIE chromaticity diagram (SI Figure S3), the film and crystal of BDABFN have the coordinates (0.6795, 0.3202) and (0.6799, 0.3199), respectively. These results are close to the international standard red coordinate (0.6700, 0.3300).[56]

It is worth to noting that all the fluorescent mixtures containing BDABFN are homogeneous and visually transparent "solutions" (SI Figure S4), suggesting the size of the aggregates is in the nanoscale.[57,58] Absorption spectra of mixtures (SI Figure S5) with a high f_w appear to have tails that level off in the long-wave region, a common feature observed in nanoparticle suspensions. Light-scattering measurement results

dx.doi.org/10.1021/jp303100a | J. Phys. Chem. C 2012, 116, 10541−10547

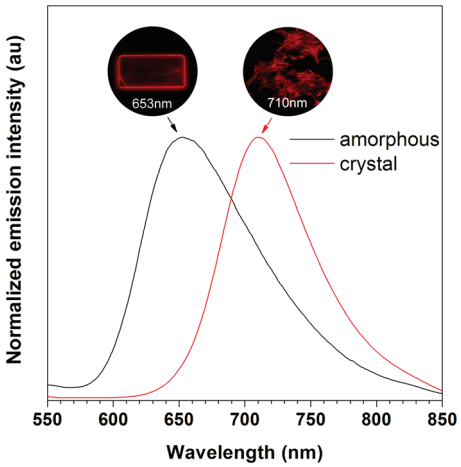

Figure 4. Normalized photoluminescence spectra of BDABFN film on quartz and crystal.

indicate the average size of the particles formed in the THF/water mixture with f_w 70% is 1504 nm. When the water fraction was increased to 80% or 90%, the particle sizes decreased to ~300−400 nm. However, when the water fraction was decreased to 60% or below, no signal could be detected. All the particle size data are listed in SI Table S2.

To get more information about the aggregates of BDABFN formed in THF/water mixtures, a scanning electron microscope (SEM) was used for morphological examination. Nanorods several hundreds of nanometers in length were observed for the cases of 80% and 90% water fraction mixtures (Figures 5A and B), whereas the nanostructures formed in 70% water fraction mixture were more regular in shape and had a larger size (Figure 5C). Nanoplates 1−2 μm in length were also found, which is in good agreement with dynamic light scattering data. Fluorescent microscopic images (Figure 5D) were also taken to investigate the morphology of BDABFN aggregates. Although the fine structure of rods was unavailable because of the lower resolution of the fluorescence microscope, the fluorescent image shows numerous optical waveguide-like emitters that exhibit strong red emission when excited at 559 nm.

The observations of high fluorescence efficiency and color purity triggered us to elucidate the molecular arrangement in the BDABFN crystal. Fortunately, a single crystal of BDABFN was obtained as dark red needles by slow evaporation from the *n*-hexane/THF mixture solution. It is assigned to a triclinic (*P*1) space group according to crystallographic data (SI Table S3). The ORTEP diagram with atom numbering scheme and some of the packing interactions in the crystal cells is depicted in Figure 6. The dihedral angle between two phenyl planes (C1−C6 and C11−C16) in the fumaronitrile part is found to be 73.88°, indicating that BDABFN is in a nonplanar conformation; neither *J*- nor *H*-aggregates are formed (Figure 6B and C). These results are quite different from the observations reported by Park and colleagues.[46] Careful analysis of the data finds that there is no evident $\pi-\pi$ stacking. Meanwhile, from further inspection of the crystal structure, however, three kinds of C−H···π hydrogen bonds with distances of 2.757−3.124 Å are formed between the hydrogen atoms of the phenyl rings in one molecule and the π cloud of the planar aromatic ring in another molecule (Figure 6B). This is a common feature of AIE active molecules.[59,60] The multiple C−H···π intermolecular interactions help rigidify the conformation and lock the intramolecular rotations of the phenyls against the central fumaronitrile unit.

CONCLUSION

In summary, we have successfully synthesized an aromatic fumaronitrile-based red fluorogen BDABFN by readily available reactions. The bromo residue can be used as a reactive site to link BDABFN with other chemical structures to prepare a series of derivatives. BDABFN shows a solid state quantum yield of

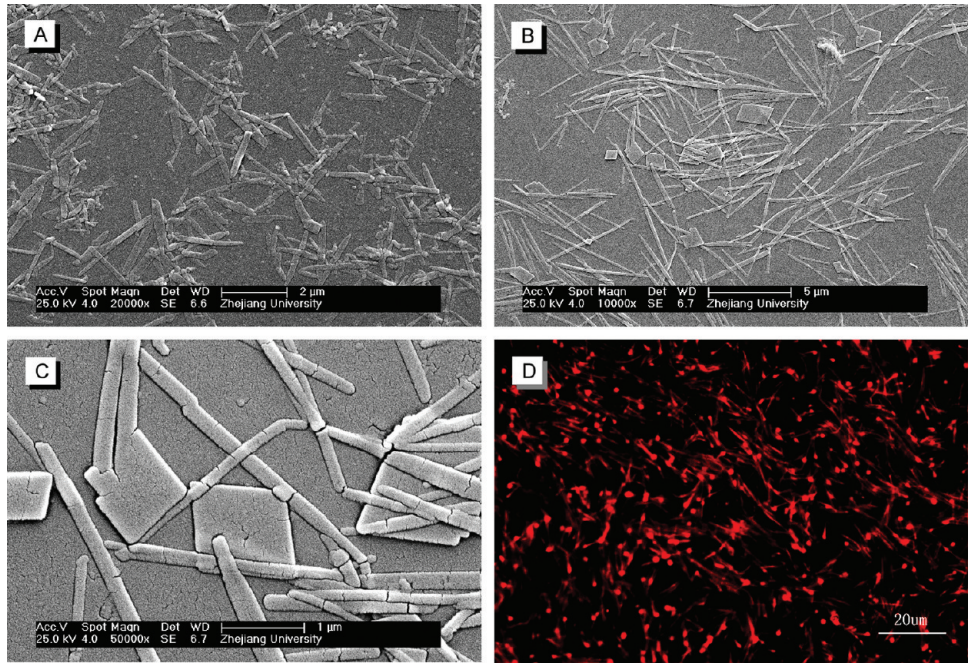

Figure 5. SEM images of nanostructures of BDABFN formed from water/THF mixture evaporation. (A) f_w = 90%. (B, C) f_w = 70%. (D) Fluorescence microscope images of BDABFN formed from water/THF mixture (f_w = 70%) evaporation. Concentration of BDABFN: 10 μM.

dx.doi.org/10.1021/jp303100a | *J. Phys. Chem. C* 2012, 116, 10541−10547

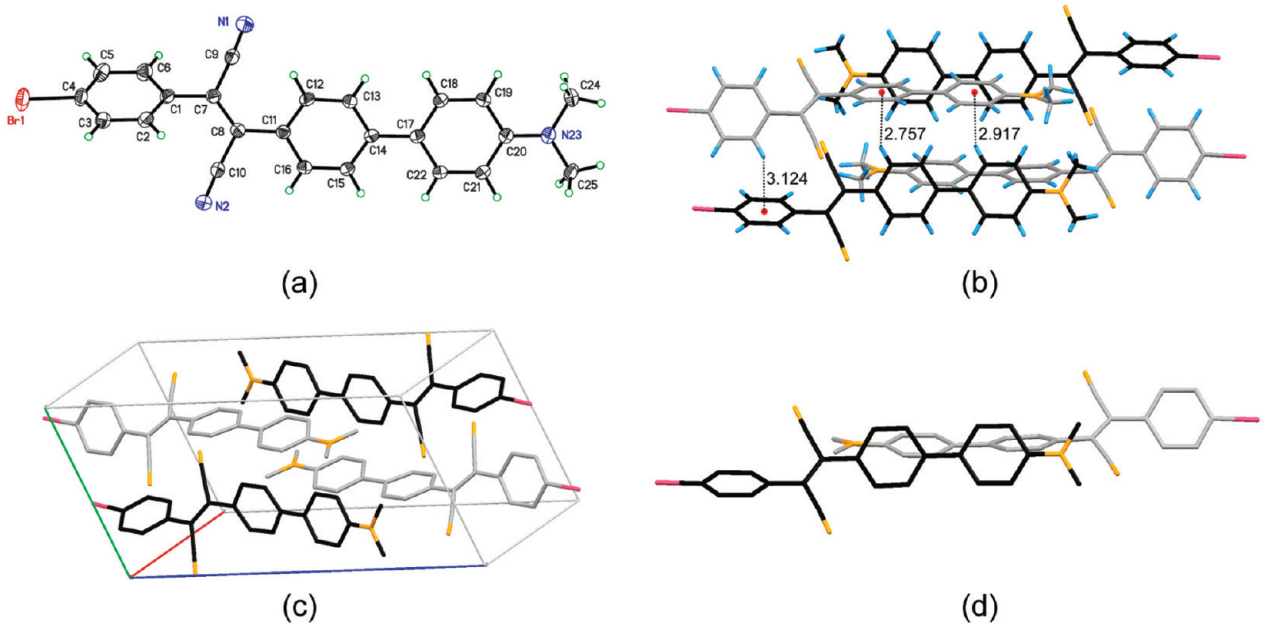

Figure 6. (a) ORTEP diagram of BDABFN, (b) C−H···π interactions in the adjacent molecules, (c) a side view of the typical packing mode of BDABFN molecules in a unit cell, and (d) a view of the adjacent molecules along the *c* direction. In c and d, the H-atoms are omitted for clarity.

26.5%. Due to the strong intramolecular interaction between the D and A units, BDABFN exhibits a pronounced positive solvatochromism with emission being tunable from yellow-green to near-IR by changing the solvent polarity from *n*-hexane to THF. TICT progress of BDABFN was also found in nonpolar/polar solvent mixtures. In a nonpolar solvent (hexane), the solution emitted strong yellow light from a low energy state. Upon addition of polar solvent (THF), the fluorescence became weaker and redder because of the TICT state. Addition of large amount of poor solvent into the THF solution of the BDABFN results in the aggregation of BDABFN molecules, which boosts their emissions through the AIE process.

Cystallographic data indicate that there is no $\pi-\pi$ stacking between the adjacent molecules, and neither *J*-aggregates nor *H*-aggregates are observed in the crystal. The existence of multiple C−H···π bonds among the adjacent molecules restricts the intramolecular rotation of the D and A moieties and enables the fluorogen to emit intensely in the solid states. Thus, both the amorphous and crystal states of BDABFN were found to emit efficient red fluorescence. With high red fluorescence quantum efficiency in solid states, high thermal stability, good flexibility of emission color tuning, and the possibility to derive new compounds, BDABFN is a promising building block to construct red-emitting materials for applications in the fields of OLEDs, biosensors, and bioimaging.

■ ASSOCIATED CONTENT

Supporting Information

Synthesis details and characterization data of BDABFN; thermal gravity analysis (TGA curve, Figure S1); theoretical calculation results of the electronic levels of BDABFN (Table S1, Figure S2); CIE chromaticity diagram of the solid film of BDABFN (Figure S3); photographs of BDABFN formed from water/THF mixtures taken under daylight and UV light (Figure S4); UV−vis absorption spectra of BDABFN formed from water/THF mixtures (Figure S5); particle sizes of BDABFN in water/THF mixtures (Table S2); crystallographic data of BDABFN (Table S3). This material is available free of charge via the Internet at http://pubs.acs.org.

■ AUTHOR INFORMATION

Corresponding Author

*(J.Z.S.) Phone: +86-571-87953734. Fax: +86-571-87953734. E-mail: sunjz@zju.edu.cn. (B.Z.T.) Phone: +852-2358-7375. Fax: +852-2358-1594. E-mail: tangbenz@ust.hk.

Notes

The authors declare no competing financial interest.

■ ACKNOWLEDGMENTS

This work was supported in part by the National Science Foundation of China (21074113 and 50873086); the key project of the Ministry of Science and Technology of China (2009CB623605), the Natural Science Foundation of Zhejiang Province (Z4110056), the Research Grants Council of Hong Kong (603509, HKUST2/CRF/10, and 604711), and the University Grants Committee of Hong Kong (AoE/P-03/08). B.Z.T. is grateful for support from the Cao Guangbiao Foundation of Zhejiang University.

■ REFERENCES

(1) Chen, C. T. *Chem. Mater.* **2004**, *16*, 4389.
(2) Allain, C.; Lartia, S. R.; Bordeau, G.; Charra, F.D. F.; Tauc, P.; Fichou, M. T. *ChemBioChem.* **2007**, *8*, 424.
(3) Shu, X.; Royant, A.; Lin, M. Z.; Aguilera, T. A.; LevRam, V.; Steinbach, P. A.; Tsien, R. Y. *Science* **2009**, *324*, 804.
(4) Zhu, B.; Jia, H.; Zhang, X.; Chen, Y.; Liu, H.; Tan, W. *Anal. Bioanal. Chem.* **2010**, *397*, 1245.
(5) Egawa, T.; Koide, Y.; Hanaoka, K.; Komatsu, T.; Terai, T.; Nagano, T. *Chem. Commun.* **2011**, *47*, 4162.
(6) Koide, Y.; Urano, Y.; Hanaoka, K.; Terai, T.; Nagano, T. *J. Am. Chem. Soc.* **2011**, *133*, 5680.
(7) Cheng, T.; Wang, T.; Zhu, W.; Chen, X.; Yang, Y.; Xu, Y.; Qian, X. *Org. Lett.* **2011**, *13*, 3656.
(8) Kobayashi, T. *J-Aggregates*, 1st ed.; University of Tokyo: Tokyo, 1996.

(9) Würthner, F.; Kaiser, T. E.; Saha-Möller, C. R. *Angew. Chem., Int. Ed.* **2011**, *50*, 3376.
(10) Baldo, M.; O'Brien, D. F.; You, Y.; Shoustikov, A.; Sibley, S.; Thompson, M. E.; Forrest, S. R. *Nature* **1998**, *395*, 151.
(11) Raymond, C.; Kwong, R. C.; Sibley, S; Dubovoy, T; Baldo, M.; Forrest, S. R.; Thompson, M. E. *Chem. Mater.* **1999**, *11*, 3709.
(12) Tao, X. T.; Miyata, S.; Sasabe, H.; Zhang, G. J.; Wada, T.; Jiang, M. H. *Appl. Phys. Lett.* **2001**, *78*, 279.
(13) Kim, D. U.; Paik, S. H.; Kim, S. H.; Tak, Y. H.; Han, Y. S.; Kim, S. D.; Kim, K. B.; Jue, H. J.; Kim, T. J. *Mater. Sci. Eng. C* **2004**, *24*, 147.
(14) Leung, M. K.; Chang, C. C.; Wu, M. H.; Chuang, K. H.; Lee, J. H.; Shieh, S. J.; Lin, S. C.; Chiu, C. F. *Org. Lett.* **2006**, *8*, 12.
(15) Barker, C. A.; Zeng, X. S.; Bettington, S; Batsanov, A. S.; Bryce, M. R.; Beeby, A. *Chem.—Eur. J.* **2007**, *13*, 6710.
(16) *Fluorescence Sensors and Biosensors*; Thompson, R. B., Ed.; CRC Press, LLC: Boca Raton, FL, 2006.
(17) *Advanced Concepts in Fluorescence Sensing*; Lakopwicz, J. R., Ed.; Springer: Norwell, 2005.
(18) Jares-Erijman, E. A.; Jovin, T. M. *Nat. Biotechnol.* **2003**, *21*, 1387.
(19) Wu, W. C.; Yeh, H. C.; Chan, L. H.; Chen, C. T. *Adv. Mater.* **2002**, *14*, 1072.
(20) Yeh, H. C.; Yeh, S. J.; Chen, C. T. *Chem. Commun.* **2003**, 2632.
(21) Luo, J.; Lam, J. W. Y.; Cheng, L.; Chen, H.; Qiu, C.; Kwok, H. S.; Zhan, X.; Liu, Y.; Zhu, D.; Tang, B. Z. *Chem. Commun.* **2001**, 1740.
(22) Dong, Y.; Lam, J. W. Y.; Qin, A.; Sun, J.; Liu, J.; Li, Z.; Sun, J.; Sung, H. H. Y.; Williams, I. D.; Kwok, H. S.; Tang, B. Z. *Chem. Commun.* **2007**, 3255.
(23) Li, Z.; Dong, Y. Q.; Lam, J. W. Y.; Sun, J.; Qin, A.; Haussler, M.; Dong, Y. P.; Sung, H. H. Y.; Williams, I. D.; Kwok, H. S.; Tang, B. Z. *Adv. Funct. Mater.* **2009**, *19*, 905.
(24) Zhao, Z. J.; Chen, S. M.; Shen, X. Y.; Mahtab, F.; Yu, Y.; Lu, P.; Lam, J. W. Y.; Kwok, H. S.; Tang, B. Z. *Chem. Commun.* **2010**, 686.
(25) Yuan, W. Z.; Chen, S. M.; Lam, J. W. Y.; Deng, C. M.; Lu, P.; Sung, H. H-Y.; Williams, I. D.; Kwok, H. S.; Zhang, Y. M.; Tang, B. Z. *Chem. Commun.* **2011**, *47*, 11216.
(26) Yu, Y.; Hong, Y.; Feng, C.; Liu, J.; Lam, J. W. Y.; Faisal, M.; Ng, K. M.; Luo, K. Q.; Tang, B. Z. *Sci. China Ser. B* **2009**, *52*, 15.
(27) Yu, Y.; Feng, C.; Hong, Y. N.; Liu, J. Z.; Chen, S. J.; Ng, K. M.; Luo, K. Q.; Tang, B. Z. *Adv. Mater.* **2011**, *23*, 3298.
(28) Hong, Y.; Haussler, M.; Lam, J. W. Y.; Li, Z.; Sin, K. yK.; Dong, Y.; Tong, H.; Liu, J.; Qin, A.; Renneberg, R.; Tang, B. Z. *Chem.—Eur. J.* **2008**, *14*, 6428.
(29) Dong, Y.; Lam, J. W. Y.; Qin, A.; Li, Z.; Liu, J.; Sun, J.; Dong, Y.; Tang, B. Z. *Chem. Phys. Lett.* **2007**, *446*, 124.
(30) Tong, H.; Hong, Y.; Dong, Y.; Haussler, M.; Lam, J. W. Y.; Li, Z.; Guo, Z.; Guo, Z.; Tang, B. Z. *Chem. Commun.* **2006**, 3705.
(31) Wang, M.; Zhang, D.; Zhang, G.; Tang, Y.; Wang, S.; Zhu, D. *Anal. Chem.* **2008**, *80*, 6443.
(32) Liu, Y.; Deng, C. M.; Tang, L.; Qin, A. J.; Hu, R. R.; Sun, J. Z.; Tang, B. Z. *J. Am. Chem. Soc.* **2011**, *133*, 660.
(33) Liu, Y.; Qin, A. J.; Chen, X. J.; Shen, X. Y.; Tong, L.; Hu, R. R.; Sun, J. Z.; Tang, B. Z. *Chem.—Eur. J.* **2011**, *17*, 14736.
(34) Wang, J.; Mei, J.; Yuan, W. Z.; Lu, P.; Qin, A. J.; Sun, J. Z.; Ma, Y. G.; Tang, B. Z. *J. Mater. Chem.* **2011**, *21*, 4056.
(35) Chen, J.; Law, C. C. W.; Lam, J. W. Y.; Dong, Y. P.; Lo, S. M. F.; Williams, I. D.; Zhu, D.; Tang, B. Z. *Chem. Mater.* **2003**, *15*, 1535.
(36) Hong, Y.; Lam, J. W. Y.; Tang, B. Z. *Chem. Commun.* **2009**, 4332.
(37) Liu, J.; Lam, J. W. Y.; Tang, B. Z. *J. Inorg. Organomet. Polym. Mater.* **2009**, *19*, 249.
(38) Wang, M.; Zhang, G.; Zhang, D.; Zhu, D.; Tang, B. Z. *J. Mater. Chem.* **2010**, *20*, 1858.
(39) Hong, Y.; Lam, J. W. Y.; Tang, B. Z. *Chem. Soc. Rev.* **2011**, *40*, 5361.
(40) Yuan, W. Z.; Lu, P.; Chen, S. M.; Lam, J. W. Y.; Wang, Z. M.; Liu, Y.; Kwok, H. S.; Ma, Y. G.; Tang, B. Z. *Adv. Mater.* **2010**, *22*, 1.
(41) Zhao, Z.; Chen, S.; Lam, J. W. Y.; Lu, P.; Zhong, Y.; Wong, K. S.; Kwok, H. S.; Tang, B. Z. *Chem. Commun.* **2010**, *46*, 2221.
(42) Zhao, Z. J.; Lu, P.; Lam, J. W. Y.; Wang, Z. M.; Chan, C. Y. K.; Sung, H. H. Y.; Williams, I. D.; Ma, Y. G.; Tang, B. Z. *Chem. Sci.* **2011**, *2*, 672.
(43) Zhao, Z. J.; Chen, S. M.; Lam, J. W. Y.; Wang, Z. M.; Lu, P.; Mahtab, F.; Sung, H. H. Y.; Williams, I. D.; Ma, Y. G.; Kwok, H. S.; Tang, B. Z. *J. Mater. Chem.* **2011**, *21*, 7210.
(44) Zhao, Z.; Deng, C.; Chen, S.; Lam, J. W. Y.; Qin, W.; Lu, P.; Wang, Z.; Kwok, H. S.; Ma, Y. G.; Qiu, H. Y.; Tang, B. Z. *Chem. Commun.* **2011**, *47*, 8847.
(45) Zhao, Q.; Zhang, S.; Liu, Y.; Mei, J.; Chen, S.; Lu, P.; Qin, A.; Ma, Y.; Sun, J. Z.; Tang, B. Z. *J. Mater. Chem.* **2012**, *22*, 7387.
(46) An, B.-K.; Kwon, S.-K.; Jung, S.-D.; Park, S. Y. *J. Am. Chem. Soc.* **2002**, *124*, 14410.
(47) Kim, D. U.; Paik, S. H.; Kim, S. H.; Tsutsui, T. *Synth. Met.* **2001**, *123*, 43.
(48) Liu, Y.; Tao, X. T.; Wang, F. Z.; Dang, X. N.; Zou, D. C.; Ren, Y.; Jiang, M. H. *J. Phys. Chem. C* **2008**, *112*, 3975.
(49) Lee, Y. T.; Chiang, C. L.; Chen, C. T. *Chem. Commun.* **2008**, 217.
(50) Mei, J.; Wang, J.; Sun, J. Z.; Zhao, H.; Yuan, W. Z.; Deng, C.; Chen, S.; Sung, H. H. Y.; Lu, P.; Qin, A.; Kwok, H. S.; Ma, Y.; Williams, I. D.; Tang, B. Z. *Chem. Sci.* **2012**, *3*, 549.
(51) Mei, J.; Wang, J.; Qin, A.; Zhao, H.; Yuan, W.; Zhao, Z.; Sung, H. H. Y.; Deng, C.; Zhang, S.; Williams, I. D.; Sun, J. Z.; Tang, B. Z. *J. Mater. Chem.* **2012**, *22*, 4290.
(52) Lippert, E. *Z. Naturforsch. A: Phys. Sci.* **1955**, *10*, 541.
(53) Mataga, N.; Kaifu, Y.; Koizumi, M. *Bull. Chem. Soc. Jpn.* **1956**, *29*, 465.
(54) *Principles of Fluorescence Spectroscopy*; Lackowicz, J. R., 3rd ed.; Springer, New York, 2006.
(55) Hu, R. R.; Lager, E.; Aguilar-Aguilar, A.; Liu, J. Z.; Lam, J. W. Y.; Sung, H. H. Y.; Williams, I. D.; Zhong, Y. C.; Wong, K. S.; Pena-Cabrera, E.; Tang, B. Z. *J. Phys. Chem. C* **2009**, *113*, 15845.
(56) Liang, C. H.; Chang, Y. C.; Chang, Y. S. *Appl. Phys. Lett.* **2008**, *93*, 211902.
(57) Liu, H.; Xu, J.; Li, Y.; Li, Y. *Acc. Chem. Res.* **2010**, *43*, 1496.
(58) Kanaparthi, R. K.; Sarkar, M.; Samanta, A. *J. Phys. Chem. B* **2009**, *113*, 15189.
(59) Dong, Y. Q.; Lam, J. W. Y.; Qin, A. J.; Liu, J. Z.; Li, Z.; Tang, B. Z. *Appl. Phys. Lett.* **2007**, *91*, 11111.
(60) Xu, J. L.; Liu, X. F.; Lv, J.; Zhu, M.; Huang, C. S.; Zhou, W. D.; Yin, X. D.; Liu, H. B.; Li, Y. L.; Ye, J. P. *Langmuir* **2008**, *24*, 8.